ISSN: 0974-5823 Vol. 7 No. 3 March, 2022

International Journal of Mechanical Engineering

Utilization of Phase Change Material (PCM) and Cuo Nanofluids in Pyramidal Solar Stills

D.Srinivas[1] and AVSSKS Gupta[2]

[1]Research scholar, Centre for Energy Studies, JNTUH College of Engineering, Kukatpally, HYDERABAD-500085.

[2]Professor, Department of Mechanical Engineering, JNTUH college of Engineering, Kukatpally, HYDERABAD-500085

Abstract - When it comes to extracting drinking water from salty and brackish water, solar powered distillation still plays a decisive role in the current scenario. The limited supply of fresh water provisions and the amount of polluted water available for potential conversion interested in drinking water using solar power are driving forces behind this article. The goal of this thesis was to improve the production of solar stills. A distillation system was created to achieve this purpose, which consists of a square pyramidal glass put on top of a black-coated aluminum sink. Solar radiation strikes the dark-skinned basin, heating and boiling the water, resulting in steam that condensate into drinkable water on the fiber glass cover. The distillation scheme is functioned at different water depths viz. 5cm and 10cm, together using PCM and CuO, for reviewing the effects of still, the filtration system is functioning at dissimilar depths of 10 cm, together with PCM and preheated water, Cuo nanoparticle is used as storage material because of its feasible thermal and economic properties. The experimental arrangement is at a 500C tilt from horizontal. Solar stills with PCM have a 162% increased hourly production on bright days. The efficiency of the still increases by 85% when it is performed with PCM, Nano particles Cuo at a penetration of 10cm, according to the results of the experiment.

Index Terms - Distillation system, Solar System, PCM, Solar Still, Nano Particle (CuO)

INTRODUCTION

Distillation technology has been used in terrestrial plants and on crafts for nearly a century to provide water to a variety of waters [1]. One of the many water purification processes is refinement, and sunlight is one of the many types of thermal energy that can be employed in this process [2]. Daylight has the advantage of not requiring any fuel, although it does necessitate additional holes (for collecting) and is still reasonably clean [3]. For the manufacture of desalinated water using solar energy, solar stills have been extensively explored and tried. Even with optimal working conditions, the reported effectiveness of a single tank solar system was between 35 and 48% in maximum cases, with less than 5L/m2/ day of fresh water production [4]. This small productivity is largely due to the ample loss of sensitivity to water vapor formation in the sun-facing, immobile glass cover [5]. To improve desalinated water production, solar stills have been used with multiple effects, but only to a limited extent, since the condenser has been indispensable portion of alembic [6]. This form of minimal mass and heat mobility coefficient nonetheless necessitates movement at somewhat high temperatures, necessitating the employment of vast and expensive metal surfaces for indulgence and construction [7]. A still oriented to the sun, with its lower profitability, cannot contest by other purification procedures [8]. It uses the similar procedures found to harvest precipitation, specifically vanishing and accumulating. Still image development based on the sun can be effectively represented as a succession; a rectilinear lid surrounds a bowl of salty water, this development heats the water, which leads to its disappearance and accumulates inside the rectilinear inclined lid [9]. The filtered water is produced has been mostly drinkable; however, the nature of the distillate is complicated because all of the inorganic and organic salts, sections, and organisms are released in the showering. In any event, the water temperature increases enough to kill all dangerous bacteria in sensitive daylight settings. A film or coating of sludge is likely to accumulate on the tank's bottom, which should be removed as often as possible [10]. Taking the eventual goal of evaporating 1 kilogramme of water at 30oC into mind, around 2.4OE106 J. is required. Aimed at a sun directed energy of 250 W/m2 and a discovered essential value of duration of 24 hours, this energy capacity disappears up to 9 L/m2/day. By and large, even despite the heat disaster, the normal solar efficiency is still around 4 5 L/m2/day. Single-impact solar-powered stills that are currently best-in-class have a proficiency of 30-40%. Users' everyday drinking water specified frequency range from 2 to 8 litres per person, whereas the typical requirement for refined water is 5 litres per person per day; hence, each human requires around 2m2 of still [11].

FIGURE 1

EXPERIMENTAL SETUP OF SQUARE PYRAMID SOLAR DISTILLATION SYSTEM

PHASE CHANGING MATERIALS

PCM is a substantial able to store, releasing large amounts of energy at a specified temperature while melted and reforming [8]. Heat is captivated when a substance deviated from solid to liquid also it released when substance transitions after liquid to solid. PCMs are sometimes known as "latent heat systems" as a result of this. Paraffin wax was used as a PCM because it was readily available and inexpensive. These temperatures have risen as a result of sun light penetrating through the glass cover and also being collected by the PCM and basin.

As wax balls are heated until the PCM spreads its temperature of fusion, heat is stored as sensible heat. Sensible heat is the quantity of energy a substance collects or releases as a result of a temperature change. The PCM starts to liquify, heat is stored as sensible heat in the melted PCM once it has completely melted [13]. As the solar radiation declines, the components of the still begin to cool. Until it completely freezes, the liquid PCM delivers heat to the basin liner and from the basin liner to the basin water. As a result, the PCM can be utilised as a source of heat during the day and night [14]. After dusk, the still keeps producing fresh water. Due to the huge quantities or high pressures necessary to store materials in their gas phase, liquid gas phase transitions are not ideal for heat storage. The heat of transformation for liquid gas transitions is higher than for solid liquid transitions [15]. Solid-state phase transitions are often gradual and have a low heat of transformation. When heat is absorbed, the temperature of the solid liquid PCMs rises, similar to that of sensible heat storage (SHS) materials. When PCMs reach the temperature at which they change phase (melting point), they absorb a substantial amount of heat at a relatively constant temperature, unlike ordinary SHS. The PCM absorbs heat by increasing its temperature until the entire material has been changed to the liquid phase. When the temperature around a liquid substance drops, the PCM hardens, releasing the latent heat it has been storing. PCMs are available in a range of temperatures ranging from 5 to 190 degrees Celsius. Traditional heat storage materials like water, masonry, and rock can only store 5 to 14 times as much heat per unit volume.

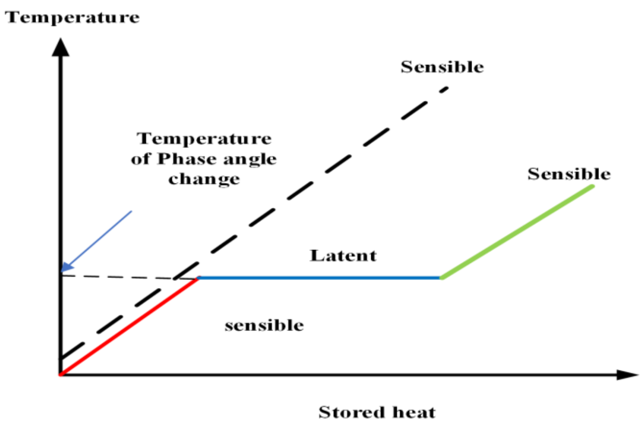

FIGURE 2

FUNCTIONAL HEAT STOWAGE IN PCM

SOLAR STILL WITH PRE HEATED WATER AND NANO PARTICLE (CUO)

On May 30th, 2021, from 8:00 to 18:00p.m., the test has been taken. The still is filled with 9.5 litres of warmed water via the supply fill inlet. The water inlet temperature is 41°C, which helps the rate of evaporation. Within 10min., the warm vapours emanating from the preheated water began to condense on the glass lid. The basin is filled with white Nanomaterials that act as a heat storage medium, extending the working time. The temperature of the water reaches a maximum of 67°C. 950 ml/m2/hr condensate was obtained during peak hour, when the coming from the sun flux was 800 W/m2. The daily output was 5.30 litres per square metre on average. Despite the fact that the sun had set and no light was shining on the basin absorber, due to the energy released by the Nano particles (Cuo), condensate was developing on the glass [12].

EXPERIMENTAL SETUP

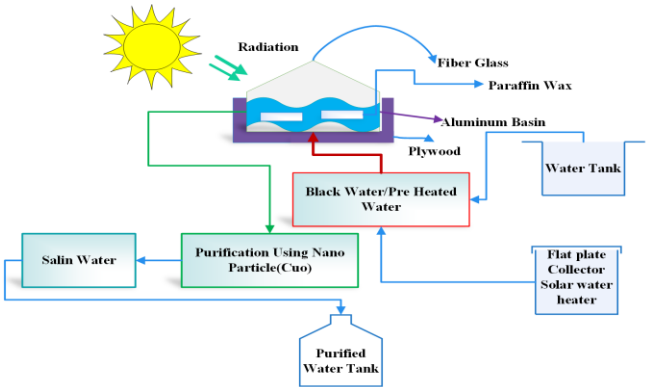

FIGURE 3

CONFIGURATION OF SQUARE PYRAMID SOLAR DISTILLATION SYSTEM

The following four stages of fabrication involved in solar still i.e.

I. Metal basin construction

Aluminum material with a thickness of 9 mm was chosen for the building of the metallic pool as it was strong thermal conduction of 215 W/mK, allows for extreme conversion of solar still into heat, which corresponds to evaporation amount of the water. The sheet is stricken and welded to form a square bucket measuring 70 cm x 70 cm, or 1m2, with a height of 15 cm and a 2 cm step at the top for square Pyramidal glass installation.

FIGURE 4

ALUMINUM BASIN

Two circular sections with a diameter of 1.5 cm for the inlet and outlet are welded on the aluminum container at opposite corners of a diagonal. For extreme absorption of solar radiation and to decrease reflection from pool, the pool is coated on the privileged with the dark paint and desiccated for two days to fully adhere to the aluminium pool.

FIGURE 5

DARK LAYERED ALUMINIUM BASIN

The pool's extreme water storing capacity is 64L. However, because water depths are limited to no more than 2 cm, the maximum fill capacity is limited to 16 litres to ensure efficient still operation.

The average temperature of the pool during the unclouded hours of the day is 58° C, enough for the water to evaporate.

The outer area of the metal cuvette is coated entirely in white to minimize radiation losses from the cuvette and the outer limits are covered in black with heats up, causing an rising measure of the airflow that can increase the rate of condensation like glass. lower the temperature.

II. Fiberglass Square Pyramid Design s

To fit pyramid inside the Al basin, the fiberglass piece is cut into four symmetrical triangular pieces of comparable size which is indicated in Figure 6 in respect to the basin. Introduction the four triangular plates on the basin, which is at a slope of 50°C, creates the pyramid shape. The 4-triangular panels joined with silicone sealants and gums. To boost machine-driven strength, four aluminum are joined to all sides of pyramid.

FIGURE 6

THE SQUARE PYRAMID IS MADE FROM A FIBRE GLASS SHEET SLICED INTO FOUR TRIANGLE FACES

The curves at foundation of the square pyramid are secured to the wood-made frame and sealed, allowing it to fit snugly into Al's sink. Elastic strips remain secured to all sides of the wood-made frame, as well as to the aluminium bucket, to prevent vapours from escaping.

FIGURE 7

THE ASSEMBLY OF WOODEN FRAME

FIGURE 8

III. Wood-made box

In wood-made box, an Al bowl combined by firmly fastened square pyramid fibre glass. A wood-made box with a measurement with 70 cm by 70 cm and a height of 12 cm is made from compressed wood with a thickness of 20 mm. Furrows are drawn on one side or the other of the funneling sections. Amid Al bowl and wood-made box, 3cm thick hole is left for setting the warm storing materials for inert warmth and may also be used to insert protective, materials for boosting the still's functionality.

FIGURE 9

WOODEN BOX FOR SQUARE PYRAMID SOLAR STILL

IV. Catchment channel

The catchment line is made up of 2 cm wide rectangular divider wire electric cables. The catchment channel is connected to the foundation of the square pyramid, which angles down from each corner to the power source corner, allowing condensed to movement to the available power segment.

FIGURE 10

. CATCHMENT CHANNEL INSIDE THE STILL

EXPERIMENTAL PROCEDURE

When the water level in the tub reaches the desired level, a float closes the valve automatically. A particular amount of a chemical that absorbs energy is added to the mix. Inside the solar still, two thermocouples are attached to estimate temperatures in various regions and at every one hour. The solar alembic is protected by a glass cover. Solar energy is allowed in the glass cover. Much of the solar radioactivity is captivated by the pool's black lacquered external, often known as a black liner. The intensity of sun radiation is measured using a pyranometer. Each half an hour, set temperature is recorded on the temperature display, and the intensity is measured with a pyranometer. From sunrise until sunset, the measured values are recorded. The procedure starts with pure water and then moves on to Cuo nanoparticles and hot water.

RESULTS AND DISCUSSIONS

On 29th may 2021, from 8 a.m. to 6 p.m., the experiment will take place. The still is filled with 9.5 litres of warmed water via the supply fill inlet. The water inlet temperature is 41°C, which helps the rate of evaporation. The hot vapours from the preheated water began to condense on the glass cover less than 10 minutes. The container is occupied with Nano fluids, which operate as a heat stowage medium and lengthen productive period. The water reaches a maximum temperature of 670°C. 950 ml/m2/hr condensate was reached during peak hour, when inward solar was 800 W/m2. Overall, the daily yield was 5.30 litres per square metre. Despite the fact that sun had set and it has no light impact on the basin conduction, condensate was accumulating on the glass because of the energy produced by Nano fliud (Cuo (120gm)).

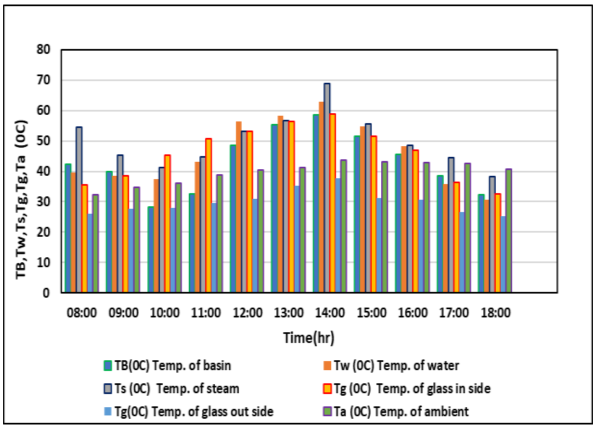

FIGURE 11

VARIATION OF TEMPERATURE IN STILL.

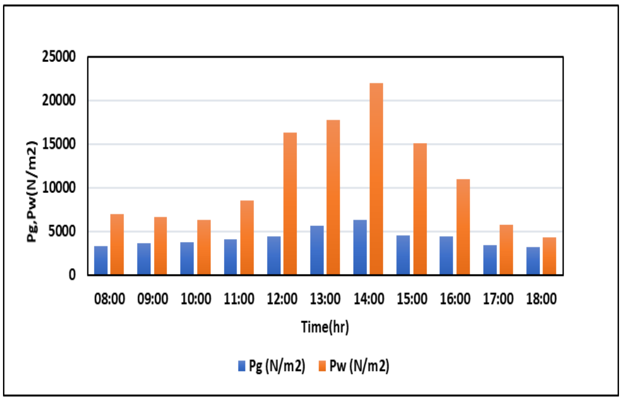

FIGURE 12

PARTIAL VAPOR PRESSURE AT GLASS AND WATER TEMPERATURE

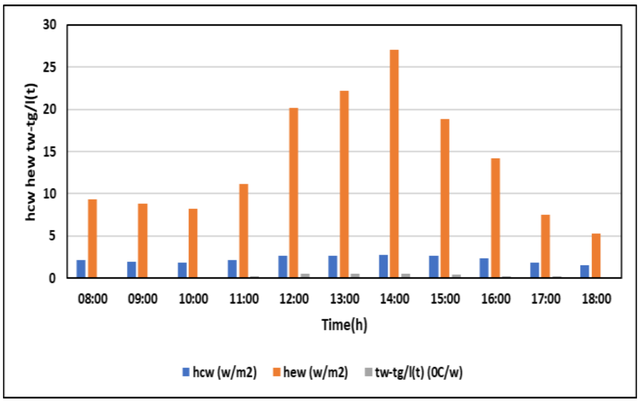

FIGURE 13

CONVECTIVE AND EVAPORATIVE HEAT TRANSFER COEFFICIENT FROM WATER TO GLASS.

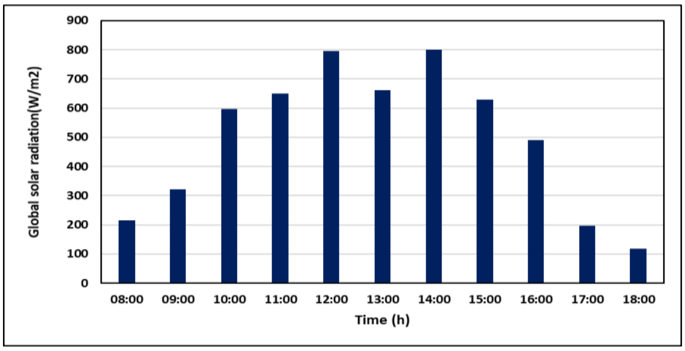

FIGURE 14

HOURLY VARIATION OF SOLAR RADIATION WITH TIME

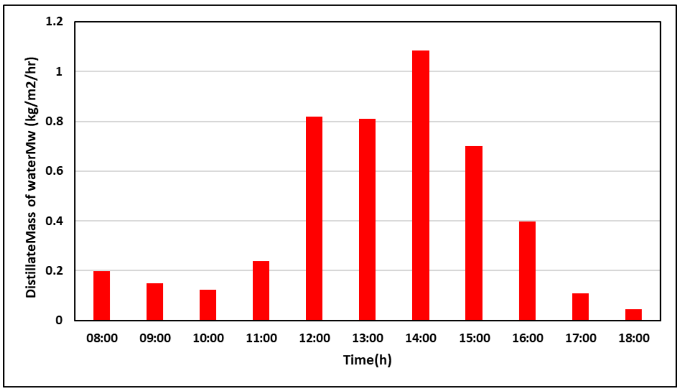

FIGURE 15

HOURLY VARIATION IN CONCENTRATE YIELD OF SOLAR STILL WITH CUO, WITH PREHEATED WATER AND WITH PCM

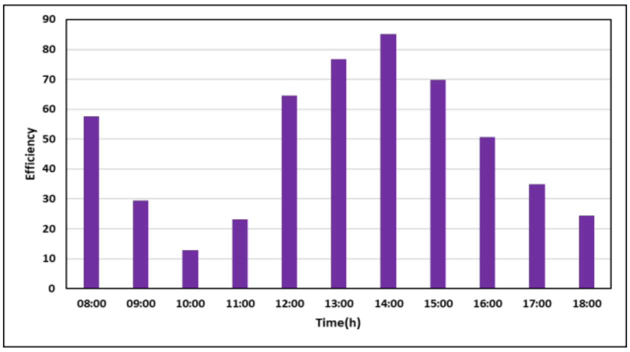

FIGURE 16

HOURLY VARIATION OF EFFICIENCY OF THE STILL WITH RESPECT TO TIME

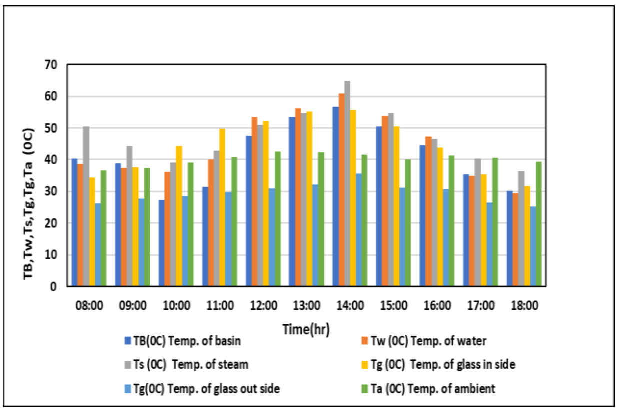

FIGURE 17

RESULTS OF VARIATION OF TEMPERATURE IN STILL

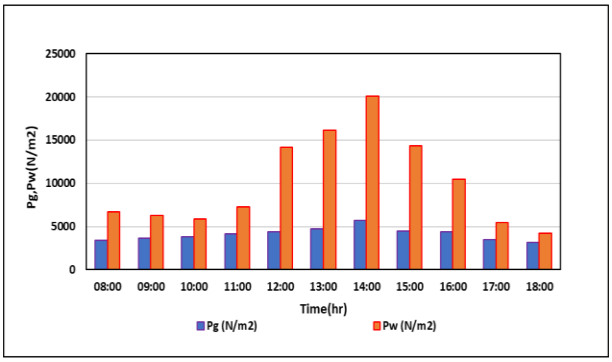

FIGURE 18

PARTIAL VAPOR PRESSURE AT GLASS AND WATER TEMPERATURE

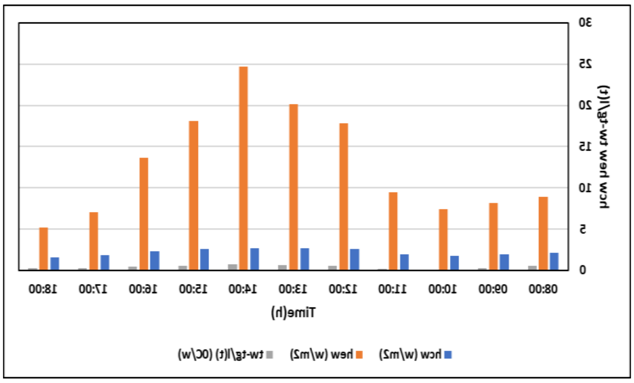

FIGURE 19

CONVECTIVE AND EVAPORATIVE HEAT TRANSFER COEFFICIENT FROM WATER TO GLASS

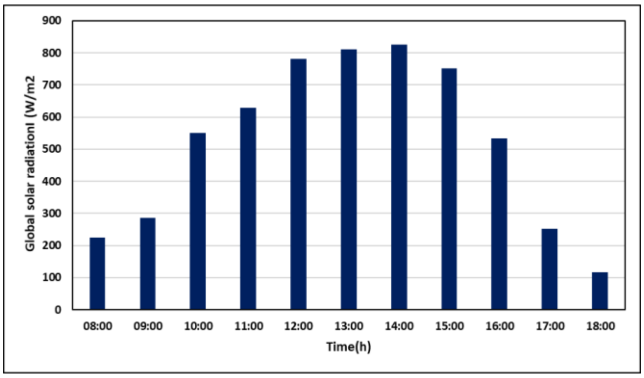

FIGURE 20

HOURLY VARIATION OF SOLAR RADIATION

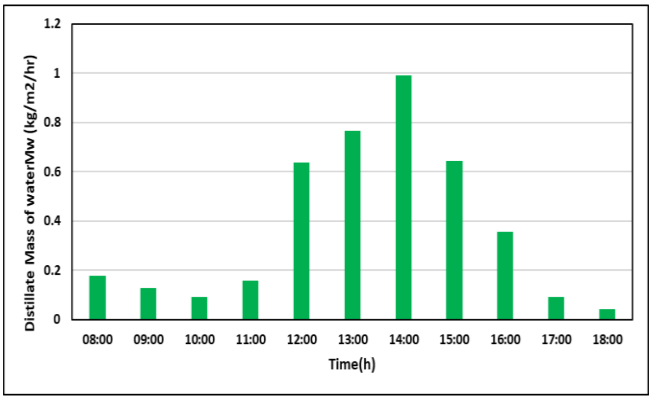

FIGURE 21

HOURLY VARIATION IN CONCENTRATE YIELD OF SOLAR STILL WITH CUO, WITH PREHEATED WATER AND WITH PCM

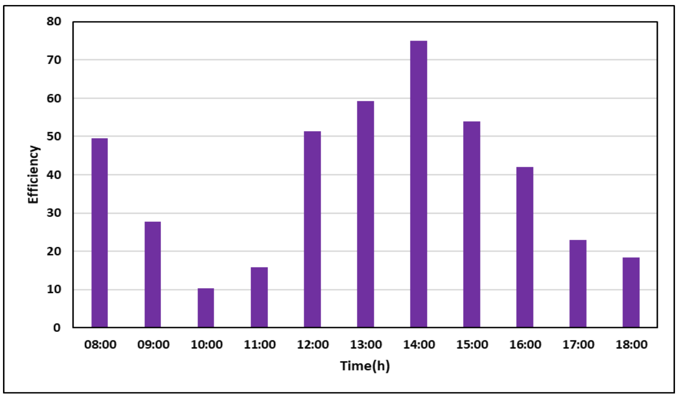

FIGURE 22

HOURLY VARIATION OF EFFICIENCY OF THE STILL

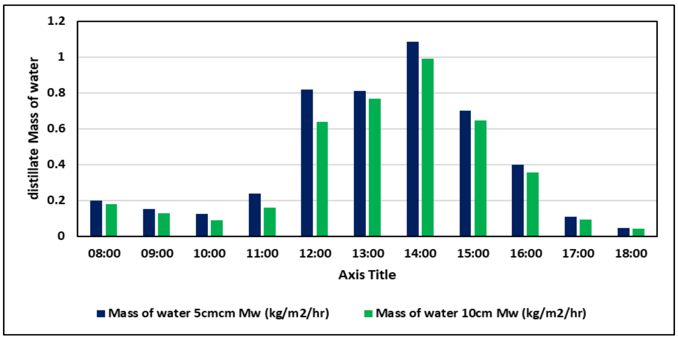

FIGURE 23

COMPARISON EFFICIENCY OF DISTILLATE WITH CUO, AND WITH PCM

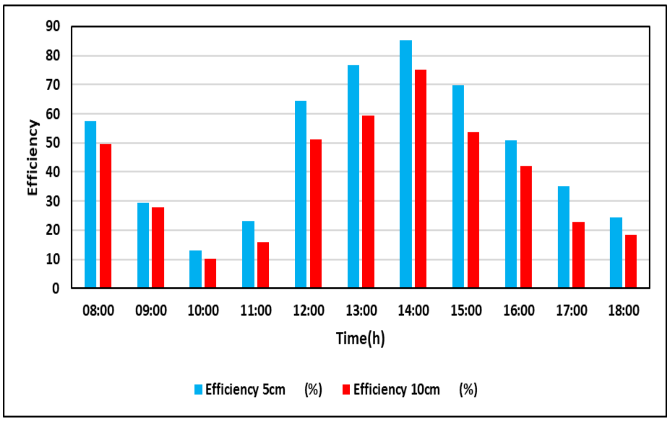

FIGURE 24

COMPARISON EFFICIENCY AT WATER DEPTH OF 5CM AND 10CM

For an average solar radiation of 500 W/m2 and duty period of 10 hours, the efficiencies obtained for solar still are tabulated below.

Table 2: Output Values for a proposed Still

S.No	Depth of water (cm)	Total amount of water ($lt/m^2/day$)	Water output ($0.95m^2$) (lt/day)	Efficiency (%)
1	5cm (Cuo)	2.65	5.30	86.24
2	10cm (Cuo)	2.15	4.30	69.96

CONCLUSION

In terms of increased distillation yield per unit area, the suggested still with PCM and Cuo offers a best promise. The solar still's performance was put to the test in terms of hidden heat stowage also different water depths. For a 5cm still alone, the condensed water collected utilising Nano particle (Cuo) is 5.30 litres/m^2/day, and 2.65 litres/m^2/day for a proposed depth still alone. The solar still with Cuo obtained 75.04% efficiency for a 10cm. The solar still's efficiency increases by 85.13 percent when the water depth is decreased by 5 cm. A nano fluid powers the proposed still, which is underwater at depth of 10cm. By assisting the evaporation rate, CuO improves the solar still's efficiency by 85 percent at a 5cm water depth. When the temperature difference between the basin liner and the glass cover is high, the still distillate production is 5.30 lifters/m^2/day.

REFERENCES

[1] I. Al-Hayeka, O.O. Badran, the effect of using different designs of solar stills on water distillation, Desalination 169 (2) (2004) 121–127.

[2] K.V. Modi, H.K. Jani, I.D. Gamit, Impact of orientation and water depth on productivity of single-basin dual-slope solar still with al2o3 and cuo nanoparticles, Journal of Thermal Analysis and Calorimetry 143 (2) (2021) 899–913.

[3] D. Dsilva Winfred Rufuss, S. Iniyan, L. Suganthi, P. Davies, Solar stills: A comprehensive review of designs, performance and material advances, Renewable and Sustainable Energy Reviews 63 (2016) 464–496.

[4] M.T. Chaichan, H.A. Kazem, Single slope solar distillatory productivity improvement using phase change material and al2o3 nanoparticle, Solar Energy 164 (2018) 370–381.

[5] Z. Haddad, A. Chaker, A. Rahmani, Improving the basin type solar still performances using a vertical rotating wick, Desalination 418 (2017) 71–78.

[6] X. Li, W.C.H. Choy, H. Lu, W.E. Sha, A.H.P. Ho, Efficiency enhancement of organic solar cells by using shape-dependent broadband plasmonic absorption in metallic nanoparticles, Advanced Functional Materials 23 (21) (2013) 2728–2735.

[7] A. Kabeel, Z. Omara, F. Essa, Improving the performance of solar still by using nanofluids and providing vacuum, Energy Conversion and Management 86 (2014) 268–274.

[8] A. Kabeel, M. Abdelgaied, Improving the performance of solar still by using pcm as a thermal storage medium under egyptian conditions, Desalination 383 (2016) 22–28.

[9] K. Khanafer, K. Vafai, A review on the applications of nanofluids in solar energy field, Renewable Energy 123 (2018) 398–406

[10] S. Nazari, H. Safarzadeh, M. Bahiraei, Performance improvement of a single slope solar still by employing thermoelectric cooling channel and copper oxide nanofluid: An experimental study, Journal of Cleaner Production 208 (2019) 1041–1052.

[11] S.S. Narayanan, A. Yadav, M.N. Khaled, A concise review on performance improvement of solar stills, SN Applied Sciences 2 (3) (2020) 1–15.

[12] S. Rashidi, N. Karimi, O. Mahian, J.A. Esfahani, A concise review on the role of nanoparticles upon the productivity of solar desalination systems, Journal of Thermal Analysis and Calorimetry 135 (2) (2019) 1145–1159.

[13] S. Rashidi, S. Akar, M. Bovand, R. Ellahi, Volume of fluid model to simulate the nanofluid flow and entropy generation in a single slope solar still, Renewable Energy 115 (2018) 400–410.

[14] S.W. Sharshir, M.A. Eltawil, A.M. Algazzar, R. Sathyamurthy, A. Kandeal, Performance enhancement of stepped double slope solar still by using nanoparticles and linen wicks: Energy, exergy and economic analysis, Applied Thermal Engineering 174 (2020).

[15] V. Vigneswaran, G. Kumaresan, B. Dinakar, K.K. Kamal, R. Velraj, Augmenting the productivity of solar still using multiple pcms as heat energy storage, Journal of Energy Storage 26 (2019)

[16] D. Krishna, M. Sasikala, and V. Ganesh, "Mathematical modeling and simulation of upqc in distributed power systems," in 2017 IEEE International Conference on Electrical, Instrumentation and Communication Engineering (ICEICE), IEEE, 2017, pp. 1–5.

[17] E. Himabindu and M. G. Naik, "Energy management system for grid integrated microgrid using fuzzy logic controller," in 2020 IEEE 7th Uttar Pradesh Section International Conference on Electrical, Electronics and Computer Engineering (UPCON), IEEE, 2020, pp. 1–6.

[18] M. Elashmawy, M. Alhadri, and M. M. Ahmed, "Enhancing tubular solar still performance using novel pcmtubes," Desalination, vol. 500, p. 114 880, 2021.

[19] D. D. W. Rufuss, S. Iniyan, L. Suganthi, and P. Davies, "Solar stills: A comprehensive review of designs, performance and material advances," Renewable and sustainable energy reviews, vol. 63, pp. 464–496, 2016.

[20] P. Boobalakrishnan, P. M. Kumar, G. Balaji, et al., "Thermal management of metal roof building using phase change material (pcm)," Materials Today: Proceedings, 2021.

Table 4: Different parameters in solar still at 5cm water depth with (Cuo 60gm

Time(h)	solar **radiation** (W/m^2)	T_B(^{0}C)	**Tw**(^{0}C)	Ts (^{0}C)	Tg (^{0}C)	Tg(^{0}C)	Ta (^{0}C)	Pg (w/m^2)	Pw (w/m^2)	**H**$_{cw}$ (w/m^2)	**H**$_{ew}$ (w/m^2)	t_w-t_g/l(t)	Mass of water	Efficiency (%)
8:00	214.645	42.4	39.5	54.4	35.5	26.2	35.5	3376.13	7017.76	2.1228	9.2997	0.5762	0.19702	57.62
9:00	321.25	39.8	38.4	45.3	38.6	27.7	37.8	3678.45	6621.34	1.9737	8.8329	0.2942	0.15055	29.42
10:00	596.26	28.3	37.5	41.2	45.4	28.1	39.2	3763.01	6311.77	1.8894	8.1968	0.1292	0.12273	12.92
11:00	650.335	32.5	43.2	44.8	50.8	29.7	41.8	4118.63	8508.45	2.142	11.1442	0.2313	0.23965	23.13
12:00	795.565	48.5	56.4	53.1	53.2	30.9	42.4	4404.49	16329.49	2.6895	20.1237	0.645	0.81741	64.5
13:00	661.15	55.4	58.2	56.7	56.3	35.3	43.3	5608.01	17775.9	2.6094	22.184	0.7683	0.80922	76.83
14:00	800.2	58.6	62.8	68.9	58.8	37.6	44.6	6345.53	21990.32	2.7215	27.0332	0.8513	1.08515	85.13
15:00	630.25	51.4	54.7	55.6	51.5	31.3	45.2	4503.58	15058.77	2.6078	18.821	0.6987	0.70154	69.88
16:00	491.2	45.5	48.3	48.5	46.8	30.8	42.8	4380.01	11015.29	2.3481	14.2448	0.5075	0.39709	50.75
17:00	197.65	38.4	35.8	44.4	36.4	26.6	41.5	3454.52	5761.59	1.8731	7.5154	0.3498	0.11013	34.98
18:00	117.31	32.3	30.6	38.3	32.6	25.2	41.8	3186.99	4331.43	1.5634	5.3013	0.244	0.0456	24.41

Table 5: Different parameters in solar still at 10cm water depth with (Cuo 120gm)

Time (h)	solar **radiation** (t) (W/m^2)	T_B(^{0}C)	**Tw** (^{0}C)	Ts (^{0}C)	Tg (^{0}C)	Tg(^{0}C)	Ta (^{0}C)	Pg (w/m^2)	Pw (w/m^2)	**H**$_{cw}$ (w/m^2)	**H**$_{ew}$ (w/m^2)	t_w-t_g/l(t)	Mass of water	Efficiency (%)
08:00	225.13	40.4	38.7	50.4	34.5	26.2	36.6	3376.13	6727.45	2.0782	8.9148	0.4949	0.1775	49.49
09:00	285.71	38.8	37.4	44.3	37.6	27.7	37.4	3678.45	6278.17	1.9089	8.1857	0.2779	0.12648	27.79
10:00	551.45	27.3	36.1	39.2	44.4	28.5	39.2	3849.27	5855.49	1.7587	7.428	0.1023	0.08992	10.23
11:00	628.71	31.5	40.2	42.8	49.8	29.7	40.8	4118.63	7280.75	1.9651	9.4687	0.1581	0.15837	15.81
12:00	780.75	47.5	53.4	51.1	52.2	30.9	42.5	4404.48	14146.12	2.5689	17.7957	0.5128	0.63781	51.28
13:00	811.01	53.4	56.2	54.7	55.3	32.3	42.3	4759.98	16175.29	2.6334	20.1245	0.593	0.76615	59.31
14:00	824.92	56.6	60.8	64.9	55.8	35.6	41.5	5699.72	20061.83	2.7068	24.6827	0.754	0.9908	75.05
15:00	750.76	50.4	53.7	54.6	50.5	31.3	40.2	4503.58	14352.33	2.5667	18.0562	0.5387	0.64427	53.86
16:00	534.46	44.5	47.3	46.5	43.8	30.8	41.4	4380.01	10478.24	2.3001	13.6014	0.4199	0.35749	41.99
17:00	251.72	35.4	34.8	40.4	35.4	26.6	40.5	3454.52	5458.06	1.8015	7.0426	0.2294	0.09199	22.94
18:00	115.76	30.3	29.6	36.3	31.6	25.2	39.3	3186.99	4259.44	1.5337	5.1602	0.2273	0.04192	18.32